WEP Warwick Evans Publishing

International Journal of Mechanical and Electrical Engineering

ISSN: 3005-9615 (Print), ISSN: 3005-7132 (Online) | Volume 2, Number 2, Year 2024
DOI: https://doi.org/10.62051/ijmee.v2n2.08
Journal homepage: https://wepub.org/index.php/IJMEE/index

Analysis and Optimization Design of U-Shaped Ironless Permanent Magnet Linear Synchronous Motor

Longqi Zhang *, Lei Zhao, Shihao Li

School of Electrical Engineering and Automation, Henan Polytechnic University, Jiaozuo Henan, China

* Corresponding Author: Longqi Zhang (Email: 1245762710@qq.com)

ABSTRACT

The working speed of the U-shaped ironless permanent magnet linear synchronous motor is determined by the frequency and pole pitch. When the motor's working speed is required to be constant, different combinations of frequency and pole pitch can be chosen. This article mainly discusses the influence of the pole pitch on the motor performance when other parameters are kept constant. First, the magnetic field of the motor permanent magnet is analyzed using the equivalent magnetizing current method to discuss the relationship between the pole pitch and the motor air gap magnetic field. Then, the finite element method is used to analyze the influence of the pole pitch on the motor air gap magnetic field, transverse edge effect, and electromagnetic thrust considering the saturation effect of the magnetic yoke. The research shows that under the conditions of constant motor basic structural parameters and speed, and the same amount of permanent magnet material, both the air gap magnetic density and the motor thrust line density have maximum values as the pole pitch changes. The research results have certain guiding significance for the design of this type of motor.

KEYWORDS

Ironless Linear Motor; Air Gap Magnetic Field; Thrust Performance; Finite Element.

1. INTRODUCTION

U-shaped ironless permanent magnet linear synchronous motor has the advantages of non-directional force, no fluting effect, small torque fluctuation, light weight, high acceleration, high positioning accuracy [1-4], and is widely used in CNC machine tools, laser cutting and other fields [5]. Due to its double-sided permanent magnet structure, this type of motor has the shortcomings of large permanent magnet consumption and low thrust density. Reasonable design can increase the thrust as far as possible under the condition of a certain motor volume and permanent magnet consumption, so as to make up for the shortcomings of the motor to a certain extent, and then better play the advantages of U-shaped ironless permanent magnet linear synchronous motor.

At present, there are many researches on the characteristics analysis and optimization of U-shaped ironless permanent magnet linear synchronous motor, most of which focus on improving motor thrust and reducing thrust fluctuation. B_y changing the winding structure, literature [6] proposes a new double-layer winding structure in which the winding is placed in layers, so that each phase coil can obtain the highest winding coefficient as possible, thus improving the thrust density. In literature [7], magnetic conductive blocks are set at both longitudinal ends of the U-shaped linear motor without iron core to make the yoke magnetic field more uniform, weaken the longitudinal end effect, and reduce the motor thrust fluctuation. Literature [8] Designed a U-shaped ironless permanent magnet

linear synchronous motor with arc permanent magnet structure, and optimized its structural parameters to greatly reduce torce ripple. In literature [9], a multi-objective optimization method with weight coefficient was proposed to optimize U-shaped coreless linear motor by using multi-population genetic algorithm to improve thrust while reducing fluctuation.

For the long secondary and short primary moving-coil ironless permanent magnet linear synchronous motor, the secondary determines the volume of the motor, and the performance of the motor mainly depends on the unit motor, so this paper only analyzes the 4-pole/3-slot unit motor. No matter how the topological structure of the motor changes, the design should ensure the constraint relationship of $v_s=2\tau f$ [10], where v_s is the synchronous speed, τ is the secondary pole pitch, and f is the current frequency. Keeping the speed unchanged, the choice of operating frequency affects the size of the motor pole pitch, which will cause the difference in the performance of U-shaped ironless permanent magnet linear synchronous motor. During the design process, the frequency changes, the pole pitch changes, other parameters remain consistent, and the motor air gap magnetic field, thrust, torce ripple, and manufacturing costs will change. Therefore, it is of great theoretical and practical significance to study the frequency selection in the design process of U-shaped ironless permanent magnet linear synchronous motor.

In this paper, the influence of the choice of different frequency and pole pitch combination on the magnetic field and thrust of the motor is studied. The effect of motor pole pitch on magnetic field of permanent magnet is analyzed, and the comparison of thrust and thrust fluctuation of motor with different pole pitch without yoke saturation and with yoke saturation is discussed. Finally, the analysis results are summarized to provide suggestions for the design of this type of motor.

2. MOTOR STRUCTURE

2.1. Motor Structure

The physical model of a unit U-shaped ironless permanent magnet linear synchronous motor is shown in Fig. 1.

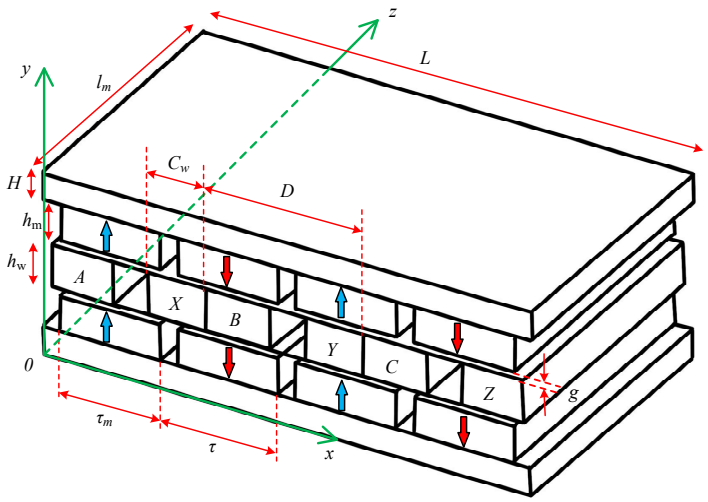

Figure 1. Structure of U-shaped ironless permanent magnet linear synchronous motor (one unit)

In the Fig.1, τ_m is the longitudinal length of the permanent magnet, l_m is the transverse width of the motor, g is the length of the unilateral air gap, H is the yoke thickness, h_m is the thickness of the permanent magnet, h_w is the winding thickness, C_w is the coil side width, D is the coil width, and L is the longitudinal length of the unit motor.

2.2. Analysis Prototype Parameters

The primary winding of each unit of the prototype adopts 4-pole/3-slot concentrated winding. The main structural parameters are shown in Table 1. In Table 1, α is the arc coefficient of the permanent magnet pole.

Table 1. Main structural parameters of U-shaped ironless linear motor

Parameter	Value
g	1 mm
l_m	50 mm
h_m	6 mm
h_w	4 mm
α	0.8
v_s	1.5 m/s

In order to achieve the operating speed of 1.5 m/s, different combinations of pole pitch and current frequency can be used. The motor model with different pole pitch is established, and the effect of pole pitch on motor performance is calculated and analyzed. The primary winding adopts a 4-pole/3-slot structure, which keeps the motor H, h_m, h_w, g and α unchanged, and C_w and τ change in the same proportion. Because the polar arc coefficients of each motor model are equal, the amount of permanent magnet is the same when the total length of the motor is the same.

A symmetrical three-phase sinusoidal current with a amplitude of 1.18A is passed through the primary winding of the motor. Take the current frequency f from 10 Hz to 70 Hz at an equal interval of 5 Hz. The motor parameters at different frequencies are shown in Table 2.

Table 2. Structural parameters of motors at different frequencies

Group number	Frequency f	Pole pitch τ	Coil width C_w
1	10 Hz	75.00 mm	40.00 mm
2	15 Hz	50.00 mm	26.67 mm
3	20 Hz	37.50 mm	20.00 mm
4	25 Hz	30.00 mm	16.00 mm
5	30 Hz	25.00 mm	13.33 mm
6	35 Hz	21.43 mm	11.43 mm
7	40 Hz	18.75 mm	10.00 mm
8	45 Hz	16.67 mm	8.89 mm
9	50 Hz	15.00 mm	8.00 mm
10	55 Hz	13.64 mm	7.27 mm
11	60 Hz	12.50 mm	6.67 mm
12	65 Hz	11.54 mm	6.15 mm
13	70 Hz	10.71 mm	5.71 mm

3. COMPARATIVE ANALYSIS OF MAGNETIC FIELD OF PERMANENT MAGNET

3.1. Magnetic Field Analysis of 2D Permanent Magnets without Considering Yoke Saturation

The structure of U-shaped ironless permanent magnet linear synchronous motor is relatively simple, and different methods can be used to analyze the permanent magnet field of the motor. Literature [11] uses the equivalent magnetizing current method to analyze the motor magnetic field. The equivalent magnetization current distribution of a permanent magnet is expressed by the function M(x) :

$$M(x)=\sum_{k=1}^{\infty}M_k\sin\left[\frac{(2k-1)\pi}{\tau}x\right],k=0,\pm1,\pm2\ldots \tag{1}$$

$$M_k=(-1)^{k+1}\frac{4}{(2k-1)\pi}M_0\sin\left[\frac{(2k-1)\pi\tau_m}{2\tau}\right] \tag{2}$$

Where,$M_0=B_r/\mu_0$, B_r is the residual magnetic induction intensity of permanent magnet, and μ_0 is the air permeability.

The expression B_y of the normal component of magnetic flux density in the gap region and the permanent magnet region is as follows [12]:

$$B_{y1}(x,y)=\sum_{k=1}^{\infty}\frac{\mu_0M_k\mathrm{sh}(m_kh_m)}{\mathrm{sh}\left(\frac{m_k\delta}{2}\right)}\cdot\sin m_kx\cdot\mathrm{ch}m_ky \tag{3}$$

$$\begin{aligned}B_{y2}(x,y)=&\sum_{k=1}^{\infty}\mu_0M_k\cdot\{-\mathrm{sh}\left[m_k\left(h_m-\frac{\delta}{2}\right)\right]\mathrm{sh}(m_ky)\\&+\mathrm{sh}\left[m_k\left(h_m-\frac{\delta}{2}\right)\right]\frac{\mathrm{ch}\left(\frac{m_k\delta}{2}\right)}{\mathrm{sh}\left(\frac{m_k\delta}{2}\right)}\mathrm{ch}(m_ky)+1\}\cdot\sin\left(m_kx\right)\end{aligned} \tag{4}$$

$$m_k=\frac{(2k-1)\pi}{\tau} \tag{5}$$

Where,$\delta=2h_m+2g+h_w$.

From formula (3), the amplitude of the v th-order harmonic of the magnetic density of the air gap can be obtained as follows:

$$B_{yv}=\frac{4B_r}{v\pi}\cdot\frac{\sin\frac{v\pi\tau_m}{2\tau}\mathrm{sh}\frac{v\pi h_m}{\tau}}{\mathrm{sh}\frac{v\pi\delta}{2\tau}} \tag{6}$$

The speed is certain, the frequency is changed during the design, the pole pitch is changed, and other parameters are consistent. The polar arc coefficients τ_m/τ, h_m and δ are fixed, and the pole pitch is changed. The variation curve of the amplitude of the normal component of the magnetic density of the air gap with the pole pitch is calculated according to equation (6), as shown in Fig. 2.

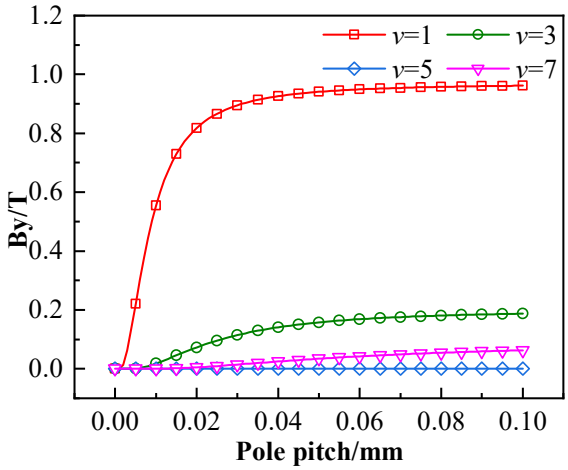

Figure 2. Amplitude variation of the normal component of air gap magnetic density with pole pitch

With the increase of the pole pitch, the amplitude of the airgap magnetic dense fundamental wave component gradually increases, and the growth rate gradually slows down. The pole pitch grows faster within 40 mm, and the amplitude of the magnetic dense fundamental wave component grows slower within 40~100 mm, which is basically unchanged. With the increase of pole pitch, the 3rd and 7th harmonics increase gradually, and the 5th harmonics approach zero.

In order to reduce the influence of partial saturation of the yoke, H=30 mm was taken for each group, ignoring the magnetic field of the armature winding. The finite element model is established and solved. The distribution waveform of the normal component of the magnetic density of the permanent magnet field in the middle of the air gap is shown in Fig. 3(a). Only the analysis results of groups 1, 5, 9 and 13 are given for easy observation and comparison.

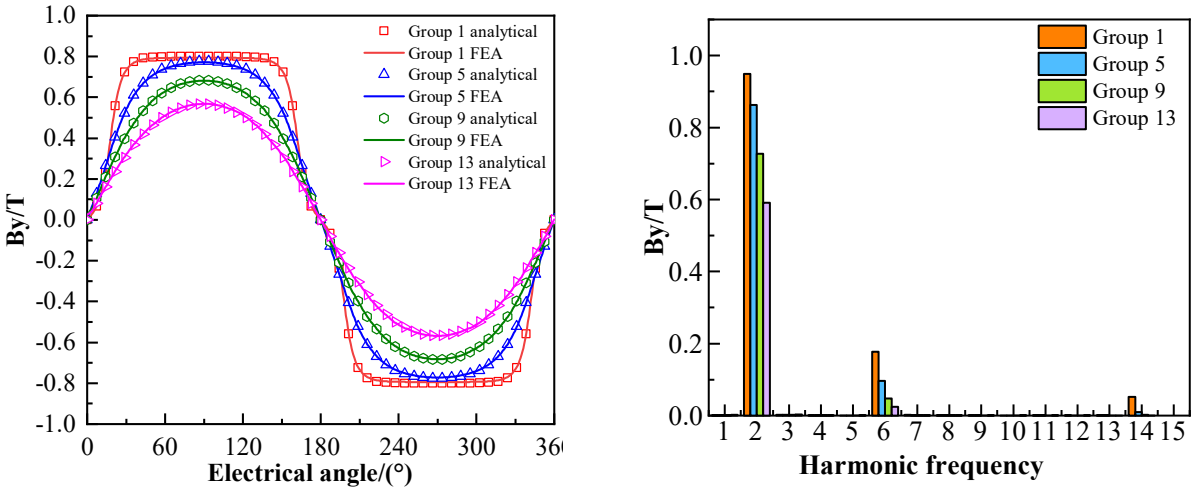

(a) Air gap field density (b) Fourier decomposition

Figure 3. Analysis of permanent magnetic field magnetic density and harmonics in air gap

With the increase of the pole pitch, the amplitude of the air gap magnetic density B_y gradually increases, but the sinusoidal property of the waveform gradually becomes worse. Group 1 in Fig. 3(a) shows that the air gap magnetic density waveform is similar to the flat-top wave due to the longer longitudinal length of the permanent magnet under a pole pitch. Comparing the magnetic density amplitude of different groups, it can be seen that when the pole pitch is small, the magnetic density amplitude can be significantly increased by increasing the pole pitch. When the pole pitch is large,

the growth rate of the magnetic density amplitude of the air gap is slow, that is, the growth rate of the magnetic density amplitude of the air gap gradually decreases with the increase of the pole pitch.

The magnetic density amplitude after Fourier decomposition is shown in Fig. 3(b). Without considering the saturation of the yoke, the larger the pole pitch, the larger the amplitude of the second harmonic. The amplitudes of the 6th and 14th harmonics both increase with the increase of the pole pitch, while the amplitudes of the 10th harmonics are close to 0 and do not change with the change of the pole pitch.

3.2. Magnetic Field Analysis of 2D Permanent Magnets Considering Yoke Saturation

At present, most analyses of air gap magnetic field in literature are carried out without considering the influence of yoke saturation on the air gap magnetic field of motor [13-15]. These studies assume that the permeability of the yoke is infinite, and do not take into account the magnetic pressure drop on the flux path of the part of the yoke, which will cause calculation errors, and the errors will increase with the increase of the saturation degree of the yoke. In addition, when the pole pitch is large, the amount of permanent magnet under one pole pitch is large, and the thickness of the yoke has to be increased to make the yoke partially unsaturated, resulting in a significant increase in the volume and weight of the motor, but the increase in the magnetic density amplitude of the air gap is small.

The magnetic yoke is a ferromagnetic material, with saturation phenomenon, nonlinear permeability, uneven distribution of magnetic density in the yoke, and different parts of the saturation degree are different, so it is difficult to use the analytical method to accurately solve, so the finite element method is combined to make a comparative analysis. The influence of yoke saturation on permanent magnet field under different pole pitch is discussed. Fig. 4(a) shows the motor air gap magnetic density comparison considering saturation (H=6 mm).

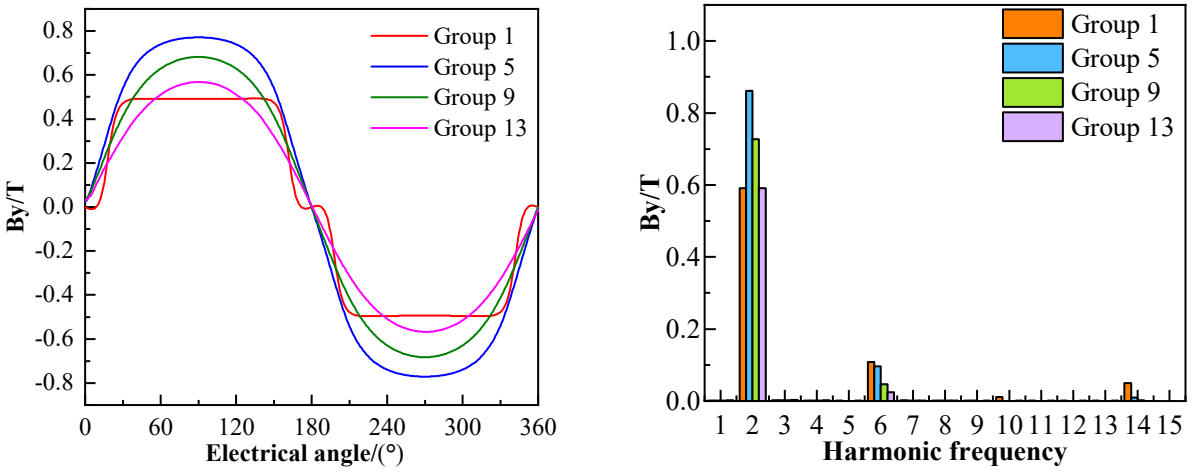

(a) Air gap field density (b) Fourier decomposition

Figure 4. Comparison of magnetic flux density considering saturation air gap of magnetic yoke

At this yoke thickness, the yoke of group 1 motor with a larger pole pitch is saturated, and the magnetic density amplitude of the same group is nearly halved compared with that of Fig. 3(a), and the waveform is distorted. Because the yoke is saturated, the magnetoresistance increases, the total magnetic flux decreases, and the effective magnetic flux of the air gap also decreases. However, the yoke of groups 5, 9 and 13 with small pole pitch is not saturated, and the magnetic density of the air gap is less affected.

In group 1, the second harmonic amplitude of the air gap flux density is greatly affected by saturation, and the sixth harmonic amplitude decreases slightly, the 10th harmonic amplitude increases slightly, and the 14th harmonic amplitude remains basically unchanged. The comparison of each harmonic

amplitude is shown in Fig. 4(b). Compared with the yoke unsaturated condition discussed in 2.1, the corresponding amplitude of the second harmonic decreases and the proportion of the higher harmonic increases, resulting in the decrease of the magnetic density amplitude of the first group and the waveform distortion. The remaining three groups of motors are less affected by saturation, and the amplitude of each harmonic is basically unchanged.

3.3. Magnetic Field Analysis of 3D Permanent Magnet Considering Yoke Saturation

In the analytical method and 2D finite element analysis, it is assumed that the transverse (along the z axis) air gap magnetic density distribution is uniform. In fact, due to the lateral edge effect, the magnetic density is gradually attenuated from the transverse middle of the motor to the two edges. A 3D finite element model is established to compare the actual air gap magnetic density distribution of different groups of motors. Fig. 5 shows the 3D distribution diagram of the normal component B_y of the air gap magnetic density at one pole pitch for different groups of motors.

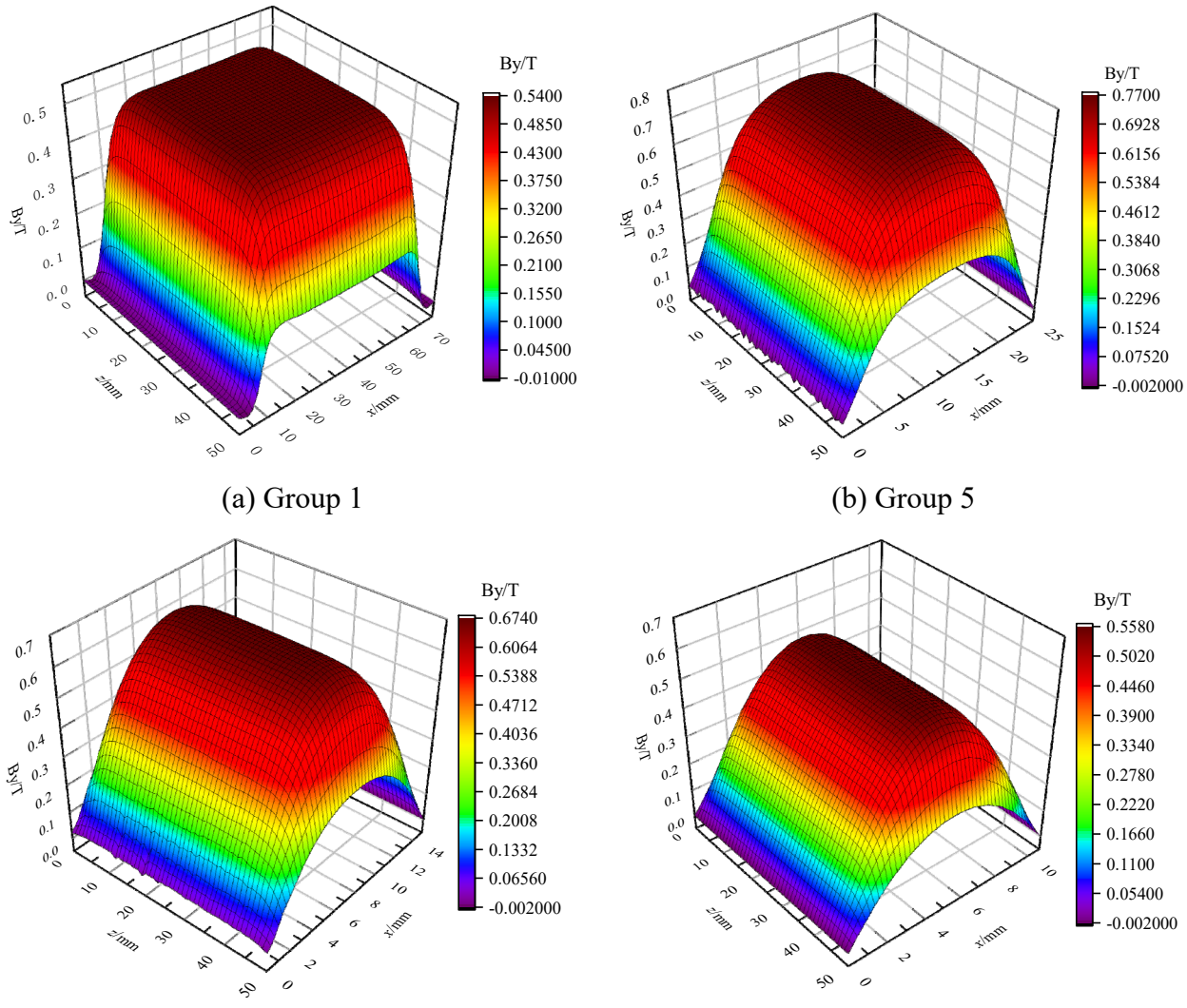

(a) Group 1 (b) Group 5

(c) Group 9 (d) Group 13

Figure 5. 3D distribution of air gap by under one pole pitch

In the3D finite element analysis, the attenuation of the magnetic density of the air gap is considered laterally, that is, the lateral edge effect. The magnetic density of the air gap gradually decreases from the transverse middle of the motor to the two edges, and the magnetic density of the air gap in the center of the motor is the highest, and the magnetic density decreases rapidly near the edge of the

motor. When the pole pitch is large, the amount of permanent magnet under one pole is large, the magnetic density waveform is flat-top, and the magnetic density amplitude is low, as shown in Fig. 5 (a). When the pole pitch is small, the proportion of magnetic leakage between electrodes in the total magnetic flux increases, and the magnetic density amplitude in the air gap decreases, as shown in Fig. 5 (c) and Fig. 5 (d). Therefore, when the pole pitch is large but the yoke saturation degree is not high, and the magnetic leakage between the poles is small, the magnetic density amplitude of the air gap is large, as shown in Fig. 5(b).

The magnetic density amplitudes of z=50 mm and z=25 mm are used to compare and analyze the effect of changing the pole pitch on the magnetic density amplitudes of the air gap at the center and the transverse edge of the motor. The comparison results of the magnetic density of the air gap in different groups are shown in Fig. 6:

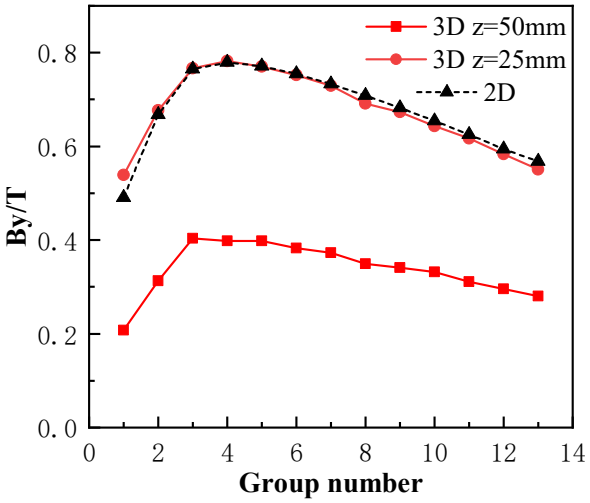

Figure 6. Comparison of magnetic density amplitudes at different positions

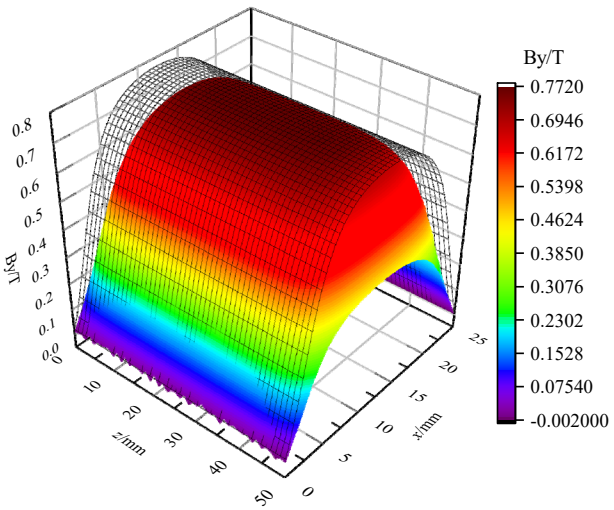

Figure 7. Comparison of 2D and 3D magnetic density distribution

With the change of pole pitch, the variation trend of the magnetic density amplitude of the air gap at the two positions of different groups of motors is basically the same, which increases first and then decreases gradually. The magnetic density in the center of the motor is higher, about 2 times that of the magnetic density at the edge of the motor, and it can be seen that the magnetic density of the air gap decreases faster at the edge of the motor. The magnetic density amplitude of the air gap in the 3D middle (z=25 mm) of each group of motors is close to that of the 2D magnetic density, and the 2D magnetic density does not consider the transverse attenuation of the air gap magnetic density. As

shown in Fig. 7, the 2D and 3D magnetic density amplitude of the air gap center is basically the same, and the closer the two edges are, the greater the gap between the magnetic density amplitude values.

3.4. Magnetic Leakage Comparison at Different Pole Pitch

The magnetic flux leakage coefficient of motor is quantitatively analyzed to reflect the leakage flux of different groups of motors. The magnetic leakage coefficient of the motor is defined as:

$$\sigma_0 = \frac{\phi_{\mathrm{m}}}{\phi_{\mathrm{g}}} \tag{7}$$

Where, ϕ_{m} is the total magnetic flux and ϕ_{g} is the effective magnetic flux of the air gap. In Fig. 8, the magnetic leakage coefficient gradually increases as the pole pitch decreases. The polar arc coefficient remains unchanged, the pole pitch decreases, the distance between two adjacent permanent magnets on the same side decreases, the magnetic leakage between the poles increases, and the leakage flux ratio increases.

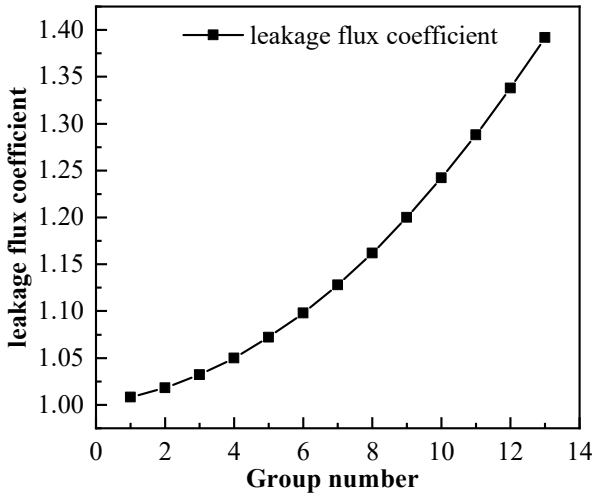

Figure 8. Comparison of leakage magnetic flux coefficients between different groups

4. COMPARATIVE ANALYSIS OF MOTOR THRUST

4.1. Motor Thrust Analysis without Considering Yoke Saturation

Expression of electromagnetic thrust generated by each phase winding of the motor [16]:

$$\begin{cases} F_{\mathrm{xA}} = \int_0^{\frac{4\tau}{3}} \int_{-\frac{h_w}{2}}^{\frac{h_w}{2}} l_{\mathrm{m}} J_{\mathrm{a}}(x) B_{\mathrm{y1}} dxdy \\ F_{\mathrm{xB}} = \int_0^{\frac{4\tau}{3}} \int_{-\frac{h_w}{2}}^{\frac{h_w}{2}} l_{\mathrm{m}} J_{\mathrm{b}}(x) B_{\mathrm{y1}} dxdy \\ F_{\mathrm{xC}} = \int_0^{\frac{4\tau}{3}} \int_{-\frac{h_w}{2}}^{\frac{h_w}{2}} l_{\mathrm{m}} J_{\mathrm{c}}(x) B_{\mathrm{y1}} dxdy \end{cases} \tag{8}$$

In the formula, lm is the effective side length of the winding, and $J_{\mathrm{a}}(x)$, $J_{\mathrm{b}}(x)$ and $J_{\mathrm{c}}(x)$ are the current density functions of the three-phase winding respectively. The resultant thrust of the three-phase winding is:

$$F_{\mathrm{x}} = F_{\mathrm{xA}} + F_{\mathrm{xB}} + F_{\mathrm{xC}} \tag{9}$$

The pole pitch changes, the corresponding unit motor length is different, solid can not directly compare the motor thrust size. In this paper, the transverse width of each motor is equal to the normal thickness of each part of the motor, so the linear thrust density of the motor is used to compare. Thrust linear density is expressed as the ratio of the average thrust of the motor to the longitudinal length of the unit motor:

$$K_{\mathrm{lf}} = \frac{F_{\mathrm{av}}}{L} \tag{10}$$

Where,F_{av} represents the average thrust of the motor.

The variation trend of the linear density of the motor thrust with the pole pitch is shown in Fig. 9:

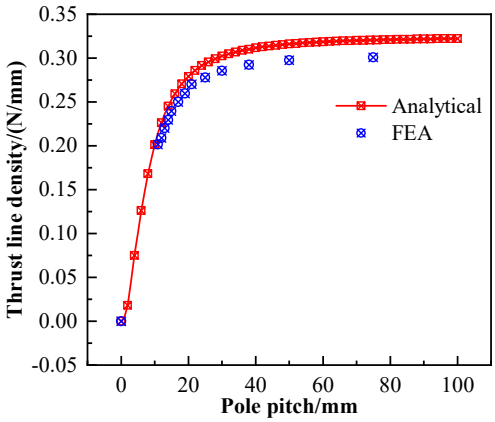

Figure 9. Curve of thrust line density with pole pitch variation

Without considering the saturation of the yoke, the thrust line density of the motor gradually increases with the increase of the pole pitch, and the growth rate gradually slows down. It can be seen that the pole pitch is within 40 mm, and the linear density of the motor thrust is greatly improved by reducing the frequency and increasing the pole pitch. However, when the pole pitch is greater than 40 mm, with the increase of the pole pitch, the increase of the thrust linear density of the motor is slow, and the effect of increasing the pole pitch by reducing the frequency is not obvious.

4.2. Motor Thrust Analysis Considering Yoke Saturation

4.2.1. Thrust Line Density Comparison

Through finite element simulation, 2D and 3D simulation results of each group of motors considering yoke saturation were compared, as shown in Fig. 10.

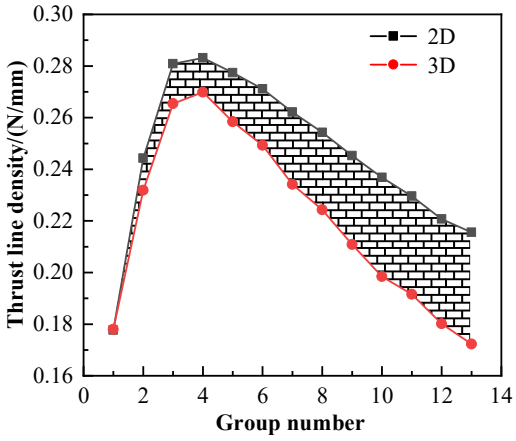

Figure 10. Comparison of thrust line density between different groups

Under the condition of yoke saturation, the thrust linear density in 2D and 3D increases first and then decreases with the decreasing of pole pitch, and reaches the maximum value in group 4. As the pole pitch decreases, the difference between 2D and 3D thrust line density gradually increases, as shown in the shaded part in Fig. 10. As the pole pitch decreases, the magnetic flux in one pole pitch length is less, the leakage flux ratio of the 3D magnetic field increases compared with the 2D magnetic field, and the thrust decreases. The difference of thrust linear density gradually increases after the thrust is unitized.

4.2.2. Comparative Analysis of Thrust Fluctuation

Thrust fluctuation is expressed as follows:

$$T_{\text{rip}} = \frac{F_{\text{max}} - F_{\text{min}}}{F_{\text{av}}} \tag{11}$$

In the formula, F_{max} and F_{min} are the maximum and minimum values of thrust respectively. As shown in Fig. 11, the finite element results of thrust fluctuation of each group of motors at different frequencies are compared.

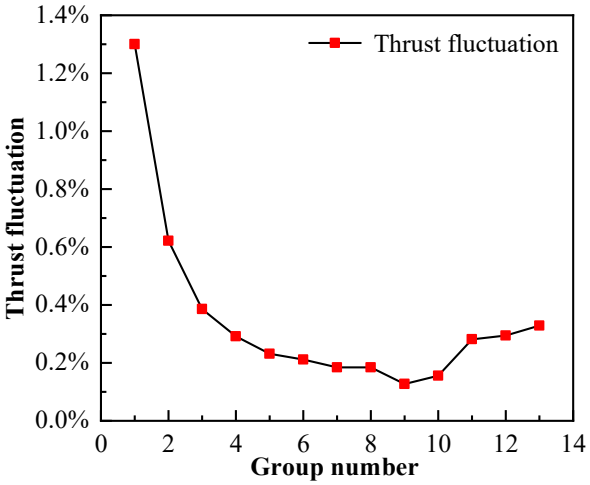

Figure 11. Comparison of torce ripple of different groups of motors

In the magnetic field analysis, the pole pitch is large, the air gap magnetic density harmonic content is high, and the waveform sinusoidal property is poor. For motors with small pole pitch, the thrust fluctuation also tends to rise as the pole pitch decreases. It can be seen that the choice of pole pitch is too large or too small, will cause the motor thrust fluctuation to a certain extent.

4.2.3. Comparative Analysis of Different Yoke Thicknesses

Through the above analysis, it can be seen that the choice of yoke thickness in the design process will affect the air gap magnetic density of the motor. When the yoke is not saturated, the increase of the thickness has little effect on the magnetic density of the air gap, which not only causes the overall weight of the motor to increase, but also causes the waste of materials and space, and the thrust is less increased. If the yoke is too thin, it is easy to supersaturate, the magnetic density amplitude of the air gap decreases rapidly, and the saturation of the yoke will cause the thrust fluctuation of the motor to increase. Keep the thickness of permanent magnet, air gap and coil the same, only change the yoke thickness, and compare the thrust linear density of each motor with different pole pitch. The results are shown in Fig. 12.

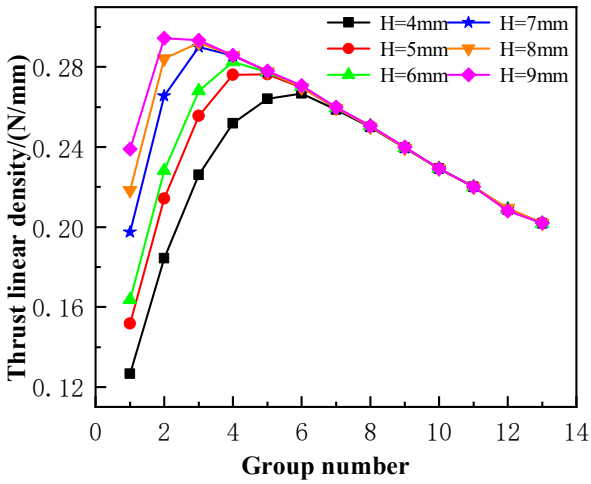

Figure 12. Comparison of thrust linear density of motor groups with different yoke thicknesses

It can be seen that with the increase of the yoke thickness, the corresponding pole pitch of the maximum thrust group motor increases gradually. That is, in the case of the same height of permanent magnets, with the increase of the thickness of the yoke, a motor with a larger pole pitch can be appropriately selected to achieve a greater thrust line density. And the maximum thrust line density increases with the increase of yoke thickness. However, when the yoke is not saturated, the yoke thickness increases and the thrust is not significantly increased. Therefore, in the design process, the yoke thickness should be selected reasonably, which can not cause saturation and decrease the thrust line density. Also can not be too thick, thrust line density does not increase and cause material and space waste.

5. SUMMARY

After the above discussion and analysis, the following conclusions can be drawn:

1) Without considering yoke saturation, the magnetic density increases gradually with the increase of pole pitch, but the growth rate decreases gradually. When the yoke is saturated, the magnetoresistance increases, and with the increase of the pole pitch, the magnetic density of the air gap first increases and then decreases, and there is a maximum value.

2) Without considering yoke saturation, thrust linear density increases gradually with the increase of pole distance, and the growth rate decreases gradually. When the yoke is saturated, the thrust line density of both 2D and 3D has a maximum value with the increase of the pole pitch. The smaller the pole pitch is, the more magnetic leakage is, and the larger the difference between the 3D thrust line density and the 2D thrust line density is.

REFERENCES

[1] LU Qinfen,SHEN Yiming,YE Yunyue. Development of permanent magnet linear synchronous motors structure and research [J]. Proceedings of the CSEE,2019,39(09): 2575-2588.

[2] KANO Y, YOSHIAKI T, KOSAKA N, et al. Simple nonlinear magnetic analysis for permanent-magnet motors [J]. IEEE Transactions on Industry Applications,2005,41(5):1205-1214.

[3] CAO Yongjuan, HUANG Yunkai, JIN Long. Design of axial-flux coreless permanent magnet brushless dc motor [J]. Journal of Southeast University (Natural Science Edition),2013,43(02):317-321.

[4] MIN S G and SARLIOGLU B. Comparative study of coreless-type pm linear synchronous machines with non-overlapping windings[C]//Energy Conversion Congress and Exposition (ECCE). USA: IEEE,2017,4274-4281.

[5] WANG Weitao,HUANG Yunkai,SONG Juncai,et al. Design and optimization of double layer reverse dip coil permanent magnet linear synchronous motors[J]. Proceedings of the CSEE,2020,40(03):980-989.

[6] MEI Weihu, LU Qinfen. Comparative analysis of an air-core pmlsm with new double-layer windings[J]. micromotors, 2019,52(05):1-5+38.

[7] QIU Shuheng,ZHANG Jie,SUN Xianbei,et al. Magnetic field optimization of u-type ironless permanent magnet linear motor using magnetic permeable block[C]// International Symposium on Linear Drives for Industry Applications (LDIA). China:IEEE,2021. 1-4.

[8] DONG Fei, ZHAO Jiwen, ZHAO Jing, et al. Thrust ripple reduction of air-core permanent magnet linear synchronous motor based on arc shaping technique and taguchi method[C]// International Electric Machines & Drives Conference (IEMDC). USA: IEEE,2019. 1169-1174.

[9] LI Liyi, TANG Yongbin, L IU Jiaxi. Design optimization of air-cored pmlsm with overlapping windings by multiple population genetic algorithm[J]. Proceedings of the CSEE,2013,33(15):69-77+14.

[10] FERKOVA Z, FRANKO M, KUCHTA J, et al. Electromagnetic design of ironless permanent magnet linear synchronous motor[C]// International Symposium on Power Electronics. Italy: IEEE,2008. 721-726.

[11] ISFAHANI A H, VAEZ-ZADEH S. Design optimization of a linear permanent magnet synchronous motor for extra low force pulsations[J]. Energy Conversion & Management,2007,48(2):443-449.

[12] LI Zheng, ZHANG Jiazhen, WANG Qunjing. Magnetic field modeling and analysis of u-shaped ironless permanent magnet linear synchronous motor[J]. Electric Machines and Control Application,2018,45(02):75-80.

[13] ZHANG Lu, KOU Baoquan, ZHAO Binchao, et al. A novel synchronous permanent magnet linear motor with halbach secondary structure[J]. Transactions of China Electrotechnical Society,2013,28(07):39-45.

[14] MOHAMMADPOUR A. Winding factor calculation for analysis of back emf waveform in air-core permanent magnet linear synchronous motors[J]. Iet Electric Power Applications,2012,6(5):253-259.

[15] VAEZ-ZADEH S, ISFAHANI A H. Multiobjective design optimization of air-core linear permanent-magnet synchronous motors for improved thrust and low magnet consumption[J]. IEEE Transactions on Magnetics, 2006, 42 (3):446-452.

[16] MIN S G and SARLIOGLU B. 3-D Performance analysis and multiobjective optimization of coreless-type pm linear synchronous motors[J]. IEEE Transactions on Industrial Electronics,2017,65(2):1855-1864.